CCL2 is a vascular permeability factor inducing CCR2-dependent endothelial retraction during lung metastasis

Marko Roblek[#1,a], **Darya Protsyuk**[#1], **Paul F. Becker**[2], **Cristina Stefanescu**[1], **Christian Gorzelanny**[3], **Jesus F. Glaus Garzon**[1], **Lucia Knopfova**[4,5], **Mathias Heikenwalder**[2,6], **Bruno Luckow**[7], **Stefan W. Schneider**[3], and **Lubor Borsig**[1]

[1]Institute of Physiology, University of Zurich and Zurich Center for Integrative Human Physiology, CH-8057 Zurich, Switzerland [2]Institute of Virology, Technische Universität München/Helmholtz Zentrum Munich, Munich, Germany [3]Department of Dermatology and Venerology, University Hospital Hamburg-Eppendorf, Hamburg, Germany [4]Department of Experimental Biology, Faculty of Science, Masaryk University, Brno, Czech Republic [5]International Clinical Research Center, Center for Biological and Cellular Engineering, St. Anne's University Hospital, Brno, Czech Republic [6]German Cancer Research Centre (DKFZ); Division of Chronic Inflammation and Cancer, Heidelberg, Germany [7]Medizinische Klinik und Poliklinik IV, Klinikum der Universität München, LMU München, Munich, Germany

[#] These authors contributed equally to this work.

Abstract

Increased levels of the chemokine CCL2 in cancer patients are associated with poor prognosis. Experimental evidence suggests that CCL2 correlates with inflammatory monocyte recruitment and induction of vascular activation; but the functionality remains open. Here, we show that endothelial Ccr2 facilitates pulmonary metastasis using an endothelial-specific Ccr2-deficient mouse model (Ccr2[ec]KO). Similar levels of circulating monocytes and equal leukocyte recruitment to metastatic lesions of Ccr2[ec]KO and *Ccr2^{fl/fl}* littermates were observed. The absence of endothelial Ccr2 strongly reduced pulmonary metastasis, while the primary tumor growth was unaffected. Despite a comparable cytokine milieu in Ccr2[ec]KO and *Ccr2^{fl/fl}* littermates the absence of vascular permeability induction was observed only in Ccr2[ec]KO mice. CCL2 stimulation of pulmonary endothelial cells resulted in increased phosphorylation of MLC2, endothelial cell retraction and vascular leakiness that was blocked by an addition of CCR2 inhibitor. These data demonstrate that endothelial CCR2 expression is required for tumor cell extravasation and pulmonary metastasis.

Implications—Findings provide mechanistic insight into how CCL2-CCR2 signaling in endothelial cells promotes their activation through myosin light chain phosphorylation resulting in endothelial retraction and enhanced tumor cell migration and metastasis.

Corresponding author: Lubor Borsig, Institute of Physiology, University of Zurich, Winterthurerstrasse 190, CH-8057 Zurich, Switzerland, Tel: +41 (44) 635-5134, Fax: +41 (44) 635-6814, lborsig@access.uzh.ch.
[a]current address: Institute of Science and Technology (IST) Austria, A-3400 Klosterneuburg, Austria

Disclosures: The authors report no conflicts of interest.

Keywords

lungs; CCR2; pMLC2; myosin

Introduction

Metastasis is the main reason for cancer-related fatalities. Hematogenous metastasis is a multistep process depending on interactions of disseminated tumor cells with the microenvironment (e.g. platelets and leukocytes) and ultimately with the endothelium in distant organs (1, 2). Tumor cell migration through vascular barriers is promoted by the recruitment of monocytic cells that contribute to formation of a metastatic niche (3–5). Pro-inflammatory chemokines, particularly CCL2, were linked to the accumulation of CCR2-expressing inflammatory monocytes during metastasis (6–9). High levels of pro-inflammatory chemokines, e.g. CCL2 and CCL5, in circulation are associated with poor prognosis for cancer patients (reviewed in 10). Therefore, many studies explored the genetic and pharmacological inhibition of the CCL2-CCR2 axis as a mean to impair monocyte recruitment to metastatic sites. Whereas CCL2 clearly potentiates monocyte recruitment *in vitro* (11), other tumor- or stroma-derived chemokines (e.g. CCL3, CCL5) may contribute to this process *in vivo* (4, 10). Similarly, inflammatory monocytes, defined as Ly6C^{hi} and CCR2$^+$ cells, express several chemokine receptors, e.g. CCR1, which can facilitate chemokine-driven monocyte recruitment to sites of inflammation or tumorigenesis (12). For instance, CCR2 was not required for inflammatory monocyte recruitment in an acute inflammation model (13, 14).

The CCL2-CCR2 chemokine/chemokine receptor axis is required for the egress of inflammatory monocytes from the bone marrow to the circulation during homeostasis and inflammation (13, 14). Thus, systemic Ccr2 deficiency or a treatment with CCL2 neutralizing agents resulted in reduced circulating monocyte numbers (8, 13). In addition, increased circulating serum levels of Ccl2 resulted in reduced responsiveness of blood cells to other chemokines (15). Similarly, anti-CCL2 antibody treatment of rheumatoid arthritis patients results in higher CCL2 serum levels and worsening of the disease symptoms (16).

There is accumulating evidence that CCR2 on stromal cells, particularly on endothelium, has a physiological role during inflammation (17, 18). Activation of brain endothelial CCR2 by CCL2 induced vascular leakiness (18) and regulated macrophage transendothelial migration (17). Furthermore, CCR2-mediated endothelial activation was linked to tumor-associated angiogenesis (19). While tumor cell-derived CCL2 expression is associated with enhanced metastasis, the analysis of metastatic lungs revealed that recruited monocytes and endothelial cells significantly contribute to an increased pool of CCL2 at metastatic sites (5). Recently, endothelial activation by CCL2 was directly linked to tumor cell-induced lung vascular permeability (9, 20); however, the underlying mechanism remains unclear.

Endothelial retraction is an essential step in metastasis both during intravasation and extravasation. Phosphorylation of VE-cadherin has been shown to be essential for initiation of transendothelial migration of leukocytes (21) and also tumor cells (5). Recent data show that VE-cadherin rearrangement in endothelial cells is associated with enhanced

phosphorylation of myosin light chain 2 (MLC2) during angiogenesis (22). In addition, inhibition of VE-cadherin rearrangement, which is associated with reduced MLC2 phosphorylation, in endothelial cells maintains endothelial barrier function during inflammation (23).

Tumor-derived chemokines actively shape the tumor microenvironment and directly affect various cell types both at primary and at metastatic sites (10, 24). Here we show that CCR2-signalling in lung endothelial cells induces cytoskeletal rearrangement resulting in enhanced vascular permeability required for monocyte-assisted tumor cell transendothelial migration and metastatic initiation.

Materials & Methods

Cell culture

Primary lung endothelial cells were isolated by immuno-magnetic selection using anti-CD31 antibody and cultivated as described previously (9). Bone marrow monocytes were isolated from femur and tibia followed by magnetic anti-CD115 purification as described previously (5). Mouse carcinoma cell lines MC-38GFP and LLC1.1 were grown as described (5). Immortalized mouse brain endothelial cell line; bEnd.3 (from ATCC) was grown in DMEM/10% FCS supplemented with 1x NEAA and 1mM Na-Pyruvate.

Mice

All animal experiments were performed according to the guidelines of the Swiss Animal Protection Law, and approved by the Veterinary Office of Kanton Zurich. C57BL/6J (wt) mice as well as systemic Ccr2-deficient mice, B6.129S4-Ccr2$^{<tm1Ifc/J>}$, were purchased from The Jackson Laboratory. *VE-cad-Cre/Ccr2$^{fl/fl}$* mouse (hereafter Ccr2^{ec}KO mouse) was generated by breeding the *Ccr2$^{fl/fl}$* mouse (25) (obtained from M. Pasparakis) with the VE-cadherin-Cre mouse, B6.FVB-Tg(Cdh5-cre)7Mlia/J, (26) (The Jackson Laboratory) in C57BL/6J background. *Ccr2$^{fl/fl}$* and Ccr2^{ec}KO littermates were used for all experiments. Mice expressing a VE-cadherin-EGFP fusion protein through a DNA construct knocked into the Cdh5 locus (27) were obtained from D. Vestweber.

Transmigration assay

Primary lung endothelial cells (3x10^4) were seeded on gelatin-coated 24-well transwell inserts with 8μm pores (BD) and allowed to grow to confluency. Endothelial cells were pre-incubated with the following inhibitors: 50 μM RS504393 (CCR2), 50 μM 2-APB (IP$_3$-gated Ca$^+$ channels), 10 μM BAPTA-AM (chelating intracellular Ca2$^+$), 1 μM ML-7 (MLCK), 5 μM H-1152 (ROCK2), 2.5 μM Blebbistatin (myosin II ATPase) for two hours in RPMI1640/10% FCS medium (all inhibitors were purchased from Tocris). The first four inhibitors were used according to manufacturer's recommendations (Tocris); for H-1152 and Blebbistatin we used concentrations as previously published (28). Upon removal of inhibitors from the endothelial cells MC-38GFP cells (2x10^4) were added in presence or absence of CD115$^+$ monocytes (1x10^5) in RPMI1640/3% FCS. Transmigration was induced with RPMI1640/10% FCS in the lower chamber and terminated after 16 hours. Alternatively, MC-38GFP cells (2x10^4) were added to the upper insert with or without

rhCCL2 (1 μg/ml; kindly provided by A. Kungl, University of Graz). The number of transmigrated MC-38GFP cells was counted using a Zeiss AxioVision microscope (n 3).

Transendothelial electrical resistance

Transendothelial electrical resistance (TEER) was measured using Electric Cell-Substrate Impedance Sensing (ECIS) as reported (29). When a constant impedance of endothelial layer was detected (24 h post-seeding) rhCCL2 (10μg/ml) was added to cells. Impedance was measured every 48 seconds (ECIS-zeta system, Applied BioPhysics Inc.) for 22 hours at a frequency of 4000Hz while cells were continuously maintained in a humidified atmosphere at 37°C and 5% CO_2. Statistical significance was calculated by unpaired t-test.

Preparation of cell lysates

Primary lung microvascular cells or bEnd.3 cells were stimulated with 40 ng/ml IL-1β (R&D Systems) for 2 hours in RPMI1640/10% FCS, and washed with PBS prior to addition of CCL2; 100 ng/ml (R&D Systems) in RPMI1640/10% FCS for indicated times. CCR2 was blocked with 50 μM RS504393 inhibitor during IL-1β and CCL2 stimulation. Cells were scraped-off the plates in ice-cold 1xPBS, centrifuged for 5 min and lysed in 100 μl cell lysis buffer (20mM Tris pH 7.5, 150mM NaCl, 1mM EDTA, 1% Triton X-100) supplemented with phosphatase inhibitor cocktail 3 (Sigma) and complete protease inhibitor cocktail (Roche) for 20 min on ice. After centrifugation, cell lysates were stored at -80°C.

Western blot

Cell lysate (20 μg) was separated on a 15% SDS-PAGE gel, transferred to a nitrocellulose membrane Protran 0.45 NC (GE Healthcare) and blocked with 5% BSA/TBS-T (1% Tween 20) for 1h at RT. Primary antibodies: rabbit anti-phosphoMLC2 (Ser19) (Cell Signaling), anti-β-catenin (Cell Signaling), anti-VE-cadherin (Abcam), and mouse anti-β-actin (Sigma) were incubated overnight at 4°C. After washing with TBS-T (3x), the membrane was incubated with a secondary antibody: HRP-linked-anti-rabbit IgG (Cell Signaling) or anti-mouse IgG, HRP-linked (Cell Signaling) for 1h at RT. After washing with TBS-T (3x), the membrane was developed with ECL West Dura solution (ThermoFisher Scientific) and chemiluminescent signal was detected using Hyperfilm ECL (GE Healthcare).

Immunoprecipitation

The endothelial cell line bEnd.3 was stimulated with 40 ng/ml IL-1β (R&D Systems) for 2h in RPMI1640/10%FCS. After washing with PBS, cells were incubated with 1 μg/ml rhCCL2 in RPMI/10%FCS for 1h. Cell lysates were prepared as mentioned above and β-catenin was immunoprecipitated with anti-β-catenin antibody overnight at 4°C in the presence of Protein G beads (GE Healthcare). Beads were washed (3x) with the lysis buffer, boiled in Laemmli buffer and separated on a 7.5% SDS-PAGE gel, followed by Western blotting.

Cell sorting of endothelial cells

Lungs of mice were perfused with PBS followed by digestion with Collagenase A and Collagenase D (2 mg/ml each, Roche) in RPMI1640/2%FCS for 1h at 37°C. The digested tissue was filtered through a 100 μm cell strainer, RBC lysed and filtered again through a 40

μm cell strainer. Resuspended cells were incubated with an F_c block (eBioscience) for 10 min in FACS buffer (PBS/10mM EDTA, 2% FCS), followed by incubation with antibodies: CD45-PB, CD11b-APC-Cy7, CD31-PE-Cy7, Ly6C-FITC, Ly6G-PerCP-Cy5.5 (all from BD) for 30 min on ice. After washing, endothelial cells (CD45⁻CD11b⁻CD31⁺) were sorted on a FACS Aria III 5L (BD).

RNA preparation, cDNA generation and qPCR

RNeasy Mini Kit (Qiagen) was used for RNA isolation from cells *in vitro* and TRI Reagent (Sigma) was used for RNA isolation from perfused lungs. cDNA was prepared from 250 ng RNA using the Omniscript RT Kit (Qiagen) according to manufacturer's instructions. Real-time PCR was performed using SYBR Green JumpStart Taq ReadyMix kit (Sigma) with gene-specific intron-spanning primers (Table S1) on the Mx3000P qPCR cycler (Agilent). Cycle conditions: 95°C for 30 sec, 60°C for 30 sec, 72°C for 30 sec. GAPDH was used as an internal control.

Flow cytometry of peripheral blood and lungs

Blood was mixed with PBS/5mM EDTA and spun down. Lung tissue was digested as described above. After RBC lysis with PharmLyse (BD), resuspended leukocytes were incubated with F_c block (eBioscience) in FACS buffer for 10 min; followed by staining with antibodies: CD45-APC-Cy7, CD11b-PE-Cy7, Ly6C-FITC, Ly6G-PerCP-Cy5.5, CD45-PerCP-Cy5.5, CD3-APC-Cy7, CD4-FITC, CD8-PE-Cy7, CD11b-BV510, CD19-APC, NK1.1-PerCP-Cy5.5, CD45-PB, anti-CD11b-APC-Cy7, anti-Ly6C-APC (all from BD) and CD146-PerCP-Cy5.5 (Biolegend) for 30 min on ice. For staining of CCR2 we used MC-21 antibody (30), followed by goat-anti-rat-PE antibodies (BD). Data were acquired with a FACSCanto (BD), in some cases with CountBright absolute counting beads (Life Technologies), and analyzed by FlowJo software (Tree Star).

Metastasis models

Lewis lung carcinoma cells LLC1.1 (300,000 cells) were subcutaneously (s.c.) injected into mice. Primary tumor was removed after 14 days and mice were terminated four weeks after s.c. injection. Perfused lungs were imaged and metastatic foci were counted. The primary tumor and the metastatic lungs were fixed and paraffin sections prepared. MC-38GFP colon cancer cells (300,000) or LLC1.1 cells (150,000) were intravenously injected (i.v.). MC-38GFP injected mice were terminated after 4 weeks and LLC1.1-injected mice after 2 weeks. Perfused lungs were imaged and metastatic foci were counted. The lungs were fixed and paraffin sections histologically evaluated.

Evans Blue assay

Ccr2^fl/fl and Ccr2^ecKO mice were s.c. injected with 300,000 LLC1.1 cells. After 14 days, 2 mg/ml of Evans Blue solution (Sigma) was i.v. injected and the lungs perfused with PBS 30 min later and analyzed (9).

Histology and immunohistochemistry

Tissue paraffin sections (2μm) were stained with hematoxylin/eosin or the following antibodies: F4/80 (Serotec), Ly6G (BD), CD31 (Abcam), CD3 (NeoMarkers), B220 (BD), Ki67 (NeoMarkers), cleaved-caspase-3 (BD). Staining was performed on a NEXES immune-histochemistry robot (Ventana instruments) using an IVIEW DAB Detection Kit (Ventana) or on a Bond MAX (Leica). Images were digitized with a SCN400 slide scanner (Leica) and analyzed using Tissue IA image analysis software in a double-blind manner (Slidepath, Leica). Tissue sections were stained simultaneously for each antigen and the signal to noise cut-off was manually adjusted for each antibody staining. This cut-off was applied to all samples within one staining group and positive signal (above the cut-off) is displayed in % of the total area analyzed.

Cytokine analysis

Cytokines in lung tissue lysates (200 μg) were measured with the ProcartaPlex Mouse Panel 1 (26-plex) kit and VEGF (10 μg lysate) with the Mouse VEGF-A Platinum ELISA kit (both eBioscience).

Statistical analysis

Statistical analysis was performed with the GraphPad Prism software (version 6.03). All data are presented as mean ±SEM and were analyzed by ANOVA with the post-hoc Bonferroni multiple comparison test. Analysis of two groups was performed with Mann-Whitney test unless stated otherwise.

Results

Characterization of mice with endothelial-specific deletion of Ccr2

To define the function of endothelial CCR2 in controlling tumor cell extravasation, we made a mouse with an endothelial cell-specific deletion of Ccr2. For this purpose the VE-cadherin-Cre mouse (26) was bred with the $Ccr2^{fl/fl}$ mouse (25) to generate the *VE-cad-Cre/ $Ccr2^{fl/fl}$* mouse (hereafter Ccr2^{ec}KO mouse). The cell-specific deletion of Ccr2 was confirmed by qPCR of sorted pulmonary endothelial cells (supplementary Figure 1A). We observed the same levels of circulating inflammatory (Ly6C^{hi}) and patrolling (Ly6C^{int}) monocytes in $Ccr2^{fl/fl}$ and Ccr2^{ec}KO mice (supplementary Figure 1B). In contrast, reduced numbers of Ly6C^{hi} monocytes were detected in $Ccr2^{-/-}$ mice as reported previously (9, 13). Other circulating leukocyte subsets were not altered between $Ccr2^{fl/fl}$ and Ccr2^{ec}KO littermates. Unchanged amount of CCR2 expression was detected on inflammatory monocytes (Ly6C^{hi}) in the peripheral blood of Ccr2^{ec}KO and $Ccr2^{fl/fl}$ mice (supplementary Figure 1C, left panel). Since VE-cadherin expression has been detected also in myeloid CD11b$^+$ cells (26), we analyzed the expression of CCR2 in knock-in mice expressing VE-cadherin-GFP from the VE-cadherin genetic locus, Cdh5-EGFP (27). We observed no GFP expression in circulating Ly6C^{hi} cells (supplementary Figure 1C, right panel). Next, we analyzed the endothelial progenitor cells (CD45$^-$CD31$^+$CD146$^+$) of the lungs (31). A reduced CCR2 expression was detected on endothelial progenitor cells from Ccr2^{ec}KO mice when compared to $Ccr2^{fl/fl}$ mice (Figure 1A). Importantly, the level of CCR2 expression on

inflammatory monocytes in Ccr2^{ec}KO mice remained unaffected (supplementary Figure 1C). Overall, these data indicate that endothelial *Ccr2* deletion does not interfere with the homeostasis of inflammatory monocytes.

Primary tumor growth is not altered by the absence of endothelial Ccr2

To assess the role of endothelial Ccr2 during tumorigenesis, mice were subcutaneously (s.c.) injected with Lewis lung carcinoma (LLC1.1) cells and spontaneous metastases to the lungs was determined. The tumor weight of dissected primary tumors was similar in all mouse genotypes after 14 days (Figure 1B). Histological analysis of primary tumors revealed no difference in the number of recruited F4/80$^+$ macrophages, Ly6G$^+$ neutrophils, CD3$^+$ T cells, and B220$^+$ B cells between *Ccr2$^{fl/fl}$* and Ccr2^{ec}KO mice (Figure 1C and supplementary Figure 1D). The number of proliferating cells (Ki67$^+$ cells), apoptotic cells (cleaved-caspase3$^+$ cells) in primary tumors was identical between both mouse genotypes. To assess the effect of endothelial CCR2-deficiency on tumor angiogenesis, we analyzed tumor vessel density, vessel area and vessel permeability (Figure 1D). We observed no differences in any of the endothelial parameters in primary tumors irrespective of endothelial CCR2 expression suggesting that overall endothelial physiology, including tumor angiogenesis, is not affected by endothelial CCR2.

The absence of endothelial Ccr2 attenuates lung metastases

After the primary tumor removal mice were terminated at 28 days post-tumor cell injection (p.i.) and spontaneous lung metastases analyzed (Figure 2A,B). We observed a significant reduction of metastases in Ccr2^{ec}KO mice, when compared to *Ccr2$^{fl/fl}$* littermates. While the number of metastases in *Ccr2$^{fl/fl}$* mice was comparable to wild-type (C57BL/6J) mice, the reduced metastases detected in Ccr2^{ec}KO mice were comparable to *Ccr2$^{-/-}$* mice. Histological analysis of lung metastases revealed no difference in the number of infiltrating macrophages (F4/80$^+$ cells), neutrophils (Ly6G+), T cells (CD3+) and B cells (B220+) between lungs from Ccr2^{ec}KO or *Ccr2$^{fl/fl}$* mice (Figure 2C, supplementary Figure 2A). Importantly, we found similar vascular density (CD31$^+$ area) within the metastatic foci in both mouse genotypes, indicating no difference in angiogenesis (Figure 2C). The number of proliferating cells (Ki67$^+$ cells) and apoptotic cells (cleaved-caspase3$^+$ cells) was equal in the metastatic foci of Ccr2^{ec}KO and *Ccr2$^{fl/fl}$* mice.

We further tested the endothelial CCR2 requirement for metastases using intravenous injection of LLC1.1 and colon carcinoma cells MC-38GFP. Experimental metastases of both cell types was significantly reduced in Ccr2^{ec}KO mice when compared to *Ccr2$^{fl/fl}$* littermates (supplementary Figure 2B,C). These results show that the absence of endothelial Ccr2 strongly attenuates the generation of pulmonary metastases.

Formation of the metastatic niche in lungs remains unaltered in Ccr2^{ec}KO mice

To test whether the endothelial Ccr2-deficiency influences the metastatic niche formation, we analyzed lungs from mice that were intravenously injected with MC-38GFP cells. Previous analysis has shown that LLC1.1 and MC-38GFP cells induce similar responses during lung metastasis (5). We observed increased recruitment of inflammatory monocytes (Ly6C^{hi} cells) at 12 h p.i. in both *Ccr2$^{fl/fl}$* and Ccr2^{ec}KO littermates (Figure 3A), which

returned to normal levels 24 h p.i., as reported previously for wt mice (9). The numbers and the recruitment kinetics of myeloid cells (CD11b$^+$), granulocytes (Ly6G$^+$), and Ly6C^{int} monocytes were similar between the two genotypes (supplementary Figure 3A).

The analysis of tumor cell-induced endothelial activation revealed an increase in E-selectin and VCAM-1 mRNA expression 12 h p.i. that was similar in both *Ccr2*$^{fl/fl}$ and Ccr2^{ec}KO littermates (Figure 3B). Serum amyloid A3 (SAA3) and S100A8 have been associated with hyperpermeable regions in metastatic lungs (20). We observed a comparable increase in the serum amyloid A expressions (SAA1, SAA2 and SAA3) in sorted endothelial cells from lungs of *Ccr2*$^{fl/fl}$ and Ccr2^{ec}KO littermates 12 h p.i. (Figure 3B). The cytokine analysis in the lungs of *Ccr2*$^{fl/fl}$ and Ccr2^{ec}KO mice at 12 h and 24 h p.i. revealed similar kinetics of cytokine expression on protein levels (Figure 3C). Chemokines (CXCL1, CCL2, CCL3, CCL7) and cytokines (GM-CSF and IL-6) associated with endothelial activation and monocyte recruitment/activation increased at 12 h p.i., and returned to normal levels at 24 h p.i. irrespective of a mouse genotype. Thus, the absence of endothelial Ccr2 has no apparent effect on leukocyte recruitment, cytokine milieu or endothelial activation in naïve or metastatic lungs.

Increased vascular permeability is dependent on endothelial Ccr2 expression

To test whether the absence of endothelial Ccr2 affects the formation of a pre-metastatic niche, we analyzed lungs of mice s.c.-injected with LLC1.1 cells at 7 and 14 days p.i. by flow cytometry. Increased recruitment of myeloid cells (CD11b$^+$), granulocytes (Ly6G$^+$), Ly6C^{int} monocytes and inflammatory monocytes (Ly6C^{hi}) to the pre-metastatic lungs was detected at day 14 in both *Ccr2*$^{fl/fl}$ and Ccr2^{ec}KO littermates (Figure 3D). Lymphoid cell recruitment remained the same irrespective of a mouse genotype (supplementary Figure 3B). Similarly, increased amounts of myeloid cell subpopulations were detected in the peripheral blood at day 14, which correlated with the primary tumor growth progression (supplementary Figure 3C).

An increase in chemokines (e.g. CXCL1, CCL7, and CCL2) in pre-metastatic lungs was observed with tumor growth progression but did not differ between *Ccr2*$^{fl/fl}$ and Ccr2^{ec}KO mice (Figure 3E). Despite reduced metastasis in the absence of endothelial Ccr2, no changes in the metastatic niche of the lungs were observed. Thus, we tested whether the lung vasculature is altered in tumor-bearing mice at 14 days. We detected small, but significant reduction in vascular permeability of Ccr2^{ec}KO mice when compared to *Ccr2*$^{fl/fl}$ littermates (Figure 3F). These findings indicate that the endothelial Ccr2 deficiency prevents induction of vascular permeability, which is required for lung metastasis.

CCL2 induces loosening of endothelial junctions and the contraction of endothelial cells

Reduced vascular permeability has been previously linked to attenuated tumor cell extravasation and metastasis (5, 9). Thus, we tested the capacity of tumor cells to migrate through pulmonary endothelial cells derived from Ccr2^{ec}KO and *Ccr2*$^{fl/fl}$ mice. Transendothelial migration (TEM) of tumor cells through wild-type endothelial cells was significantly potentiated by the addition of monocytes (Figure 4A), as described previously (9). However, TEM of tumor cells was potentiated by monocytes only through endothelial

cells derived from *Ccr2*^{fl/fl} but not from Ccr2^{ec}KO mice (Figure 4A). To identify the signaling cascade facilitating the CCL2-induced vascular permeability, we targeted the G-protein-coupled receptor pathway that is required for the actin-myosin complex activation (Figure 4B). Interestingly, the pre-incubation of endothelial cells with inhibitors of: CCR2 (RS504393), IP$_3$-receptor (2-APB), intracellular Ca^{2+} (BAPTA-AM), myosin light-chain kinase MLCK (ML-7), Rho-associated kinase ROCK (H-1152), and myosin II ATPase (Blebbistatin) significantly reduced TEM of tumor cells. Of note, endothelial cells pretreated with RS504393, ML-7, or H-1152 showed also impaired TEM of 4T1 breast cancer cells (supplementary Figure 4A). These data indicate that inhibition of endothelial retraction attenuates monocyte-assisted transendothelial migration of tumor cells. Importantly, an addition of recombinant CCL2 increased TEM of MC-38GFP cells also in the absence of monocytes (Figure 4C). Since MC-38GFP cells do not express Ccr2 (32), we tested the hypothesis that CCL2 activates endothelial CCR2 which results in endothelial retraction. We measured transendothelial electrical resistance (TEER) of primary pulmonary endothelial cells after stimulation with CCL2. TEER of the endothelial monolayer decreased upon CCL2 stimulation compared to the control (Figure 4D, supplementary Figure 4B), confirming that CCL2 stimulation triggers endothelial retraction.

Activation of actin-myosin contraction is required for cell retraction and depends on phosphorylation of myosin light chain 2 (pMLC2) (33). Stimulation of endothelial cells with CCL2 resulted in accumulation of pMLC2 (Figure 5A). The analysis of an endothelial cell line bEnd.3 showed that CCL2 activation induced the accumulation of pMLC2 1-2 hours after stimulation (Figure 5B). We observed no changes in total MLC2 expression but only an increase in MLC2 phosphorylation (supplementary Figure 5A). To prove that endothelial pMLC2 accumulation is driven by CCL2 stimulation, we treated bEnd.3 cells with a CCR2 inhibitor that resulted in diminished phosphorylation of MLC2 (Figure 5C). Loosening of the endothelial barrier is caused by the dissociation of VE-cadherin/β-catenin complex (34). CCL2 stimulation of endothelial cells resulted in dissociation of the VE-cadherin/β-catenin complex (Figure 5D) hence confirming a direct effect of CCL2 on endothelial barrier function. CCL2 activated bEnd.3 cells showed also reduced VE-cadherin co-localization with β-catenin (supplementary figure 5B-C); thereby complementing the immunoprecipitation data (Figure 5D). These data provide evidence that CCL2-driven activation of endothelial CCR2 results in the cytoskeletal rearrangement and loosening of the endothelial cell junctions and thereby facilitates an efficient transendothelial migration of tumor cells.

Discussion

Dissemination of tumor cells during metastasis is promoted by platelet- and monocyte-assisted extravasation from the circulation (3, 5, 9, 35). Particularly, the chemokine/chemokine receptor axis CCL2-CCR2 appears to be involved in several steps during metastasis including leukocyte recruitment, angiogenesis, immune suppression, and cancer cell extravasation (6–9, 35). Since the systemic inhibition of CCR2/CCL2 interferes with the egress of inflammatory monocytes from the bone-marrow (13, 36), the observed reduced recruitment of monocytes to metastatic sites is rather a consequence of reduced numbers of circulating Ly6C^{hi} cells. To dissect the contribution of endothelial Ccr2 from the Ccr2-

dependent monocyte recruitment to metastasis we generated an endothelial cell-specific Ccr2 deletion mouse model (Ccr2^{ec}KO mice). In this model, we observed no alteration in the numbers of circulating cells or in the recruitment of inflammatory monocytes to metastatic lungs. Nevertheless, a significant attenuation of metastasis was observed in Ccr2^{ec}KO mice when compared to control littermates. Taken together, these findings suggest that the local activation of endothelial Ccr2 is essential for tumor cell extravasation during lung metastasis.

Endothelial CCR2 has been linked to regulation of the blood-brain-barrier vascular permeability during inflammation (18, 37) and to the regulation of angiogenesis (38, 39). Recently we have shown that endothelial CCR2 promotes metastasis by facilitating tumor cell extravasation (9). In this report we show that neither the primary tumor growth nor the tumor angiogenesis were affected by the absence of endothelial CCR2, which is agreement with previous findings that endothelial CCR2 expression has been observed only in the brain and the lungs (9, 38). Notably, the absence of endothelial Ccr2 did not alter the endothelial activation upon tumor cell challenge.

Transendothelial migration of cells is a tightly regulated process that controls distribution of leukocytes throughout the organism (40). Induction of vascular permeability is essential for an efficient transendothelial migration of tumor cells (9, 20, 41). Enhanced vascular permeability in lungs was previously associated with a Ccr2-dependent increase of inflammatory permeability factors SAA1+2 and SAA3 (20). We observed similar cytokine and chemokine levels in lungs of tumor-challenged mice of Ccr2^{ec}KO and *Ccr2$^{fl/fl}$* genotypes. Although similar levels of permeability factors such as VEGF-A, SAA3 and CCL2 were detected in the lungs of Ccr2^{ec}KO and *Ccr2$^{fl/fl}$* mice, we observed impaired induction of vascular permeability only in Ccr2^{ec}KO mice. These results demonstrate that endothelial CCR2 is the regulator of tumor cell-induced lung vascular permeability. Furthermore, transendothelial electrical resistance was decreased by CCL2 stimulation of endothelial cells, indicating loosening and disassembly of endothelial intercellular junctions. Inhibition of CCR2 or the proteins regulating the endothelial actin-myosin cytoskeleton (MLCK, ROCKII, myosin II) severely impaired tumor cell transendothelial migration *in vitro*. In endothelial cells, MLC2 phosphorylation represents the sole regulation of myosin II ATPase activity during inflammation or angiogenesis (22, 23, 42–44). Indeed, CCL2 stimulation of endothelial cells induced phosphorylation of MLC2, which could be blocked by a CCR2 inhibitor. Presented data provide evidence that CCR2-mediated endothelial activation induces disassembly of adherens junctions thereby facilitating transendothelial migration of tumor cells.

In conclusion, we describe a mechanism how endothelial CCR2 regulates lung metastasis through the activation of the actin-myosin cytoskeleton using by an endothelial cell-specific Ccr2-deficient (Ccr2^{ec}KO) mouse model. Translation of CCR2 inhibition into clinical setting will require timely and spatially defined approach, due to the homeostatic function of CCL2-CCR2 signaling mediating the release of monocytes from the bone marrow (36). Systemic inhibition of CCL2 in mouse models led to reduction of breast cancer metastasis, however; cessation of a treatment resulted in accelerated tumor growth due to an enhanced release of monocytes from the bone marrow (8). Nevertheless, targeting of CCR2 inhibitors

to the metastatic niche attenuated metastasis without any side effects (32, 45). Further progress in cell-specific targeting will show whether CCR2 targeting will be of therapeutic value.

Supplementary Material

Refer to Web version on PubMed Central for supplementary material.

Acknowledgements

References

1. Labelle M, Hynes RO. The initial hours of metastasis: the importance of cooperative host-tumor cell interactions during hematogenous dissemination. Cancer Discov. 2012; 2:1091–9. [PubMed: 23166151]

2. Quail DF, Joyce JA. Microenvironmental regulation of tumor progression and metastasis. Nat Med. 2013; 19:1423–37. [PubMed: 24202395]

3. Qian B, Deng Y, Im JH, Muschel RJ, Zou Y, Li J, et al. A distinct macrophage population mediates metastatic breast cancer cell extravasation, establishment and growth. PLoS One. 2009; 4:e6562. [PubMed: 19668347]

4. Kitamura T, Qian BZ, Pollard JW. Immune cell promotion of metastasis. Nat Rev Immunol. 2015; 15:73–86. [PubMed: 25614318]

5. Hauselmann I, Roblek M, Protsyuk D, Huck V, Knopfova L, Grassle S, et al. Monocyte Induction of E-Selectin-Mediated Endothelial Activation Releases VE-Cadherin Junctions to Promote Tumor Cell Extravasation in the Metastasis Cascade. Cancer Res. 2016; 76:5302–12. [PubMed: 27488527]

6. Lu X, Kang Y. Chemokine (C-C motif) ligand 2 engages CCR2+ stromal cells of monocytic origin to promote breast cancer metastasis to lung and bone. J Biol Chem. 2009; 284:29087–96. [PubMed: 19720836]

7. Qian BZ, Li J, Zhang H, Kitamura T, Zhang J, Campion LR, et al. CCL2 recruits inflammatory monocytes to facilitate breast-tumour metastasis. Nature. 2011; 475:222–5. [PubMed: 21654748]

8. Bonapace L, Coissieux MM, Wyckoff J, Mertz KD, Varga Z, Junt T, et al. Cessation of CCL2 inhibition accelerates breast cancer metastasis by promoting angiogenesis. Nature. 2014; 515:130–3. [PubMed: 25337873]

9. Wolf MJ, Hoos A, Bauer J, Boettcher S, Knust M, Weber A, et al. Endothelial CCR2 signaling induced by colon carcinoma cells enables extravasation via the JAK2-Stat5 and p38MAPK pathway. Cancer Cell. 2012; 22:91–105. [PubMed: 22789541]

10. Borsig L, Wolf MJ, Roblek M, Lorentzen A, Heikenwalder M. Inflammatory chemokines and metastasis-tracing the accessory. Oncogene. 2014; 33:3217–24. [PubMed: 23851506]

11. Volpe S, Cameroni E, Moepps B, Thelen S, Apuzzo T, Thelen M. CCR2 acts as scavenger for CCL2 during monocyte chemotaxis. PLoS One. 2012; 7:e37208. [PubMed: 22615942]

12. Shi C, Pamer EG. Monocyte recruitment during infection and inflammation. Nat Rev Immunol. 2011; 11:762–74. [PubMed: 21984070]

13. Serbina NV, Pamer EG. Monocyte emigration from bone marrow during bacterial infection requires signals mediated by chemokine receptor CCR2. Nat Immunol. 2006; 7:311–7. [PubMed: 16462739]

14. Shi C, Jia T, Mendez-Ferrer S, Hohl TM, Serbina NV, Lipuma L, et al. Bone marrow mesenchymal stem and progenitor cells induce monocyte emigration in response to circulating toll-like receptor ligands. Immunity. 2011; 34:590–601. [PubMed: 21458307]

15. Cardona AE, Sasse ME, Liu L, Cardona SM, Mizutani M, Savarin C, et al. Scavenging roles of chemokine receptors: chemokine receptor deficiency is associated with increased levels of ligand in circulation and tissues. Blood. 2008; 112:256–63. [PubMed: 18347198]

16. Haringman JJ, Gerlag DM, Smeets TJ, Baeten D, van den Bosch F, Bresnihan B, et al. A randomized controlled trial with an anti-CCL2 (anti-monocyte chemotactic protein 1) monoclonal antibody in patients with rheumatoid arthritis. Arthritis Rheum. 2006; 54:2387–92. [PubMed: 16869001]

17. Dzenko KA, Song L, Ge S, Kuziel WA, Pachter JS. CCR2 expression by brain microvascular endothelial cells is critical for macrophage transendothelial migration in response to CCL2. Microvasc Res. 2005; 70:53–64. [PubMed: 15927208]

18. Stamatovic SM, Keep RF, Kunkel SL, Andjelkovic AV. Potential role of MCP-1 in endothelial cell tight junction 'opening': signaling via Rho and Rho kinase. J Cell Sci. 2003; 116:4615–28. [PubMed: 14576355]

19. Salcedo R, Ponce ML, Young HA, Wasserman K, Ward JM, Kleinman HK, et al. Human endothelial cells express CCR2 and respond to MCP-1: direct role of MCP-1 in angiogenesis and tumor progression. Blood. 2000; 96:34–40. [PubMed: 10891427]

20. Hiratsuka S, Ishibashi S, Tomita T, Watanabe A, Akashi-Takamura S, Murakami M, et al. Primary tumours modulate innate immune signalling to create pre-metastatic vascular hyperpermeability foci. Nat Commun. 2013; 4

21. Wessel F, Winderlich M, Holm M, Frye M, Rivera-Galdos R, Vockel M, et al. Leukocyte extravasation and vascular permeability are each controlled in vivo by different tyrosine residues of VE-cadherin. Nat Immunol. 2014; 15:223–30. [PubMed: 24487320]

22. Warren NA, Voloudakis G, Yoon Y, Robakis NK, Georgakopoulos A. The product of the gamma-secretase processing of ephrinB2 regulates VE-cadherin complexes and angiogenesis. Cell Mol Life Sci. 2018; 75:2813–26. [PubMed: 29428965]

23. Burg N, Swendeman S, Worgall S, Hla T, Salmon JE. Sphingosine -1 Phosphate Receptor-1 signaling maintains endothelial cell barrier function and protects against immune complex-induced vascular injury. Arthritis Rheumatol. 2018

24. Balkwill FR. The chemokine system and cancer. J Pathol. 2012; 226:148–57. [PubMed: 21989643]

25. Willenborg S, Lucas T, van Loo G, Knipper JA, Krieg T, Haase I, et al. CCR2 recruits an inflammatory macrophage subpopulation critical for angiogenesis in tissue repair. Blood. 2012; 120:613–25. [PubMed: 22577176]

26. Alva JA, Zovein AC, Monvoisin A, Murphy T, Salazar A, Harvey NL, et al. VE-Cadherin-Cre-recombinase transgenic mouse: a tool for lineage analysis and gene deletion in endothelial cells. Dev Dyn. 2006; 235:759–67. [PubMed: 16450386]

27. Winderlich M, Keller L, Cagna G, Broermann A, Kamenyeva O, Kiefer F, et al. VE-PTP controls blood vessel development by balancing Tie-2 activity. J Cell Biol. 2009; 185:657–71. [PubMed: 19451274]

28. Sadok A, McCarthy A, Caldwell J, Collins I, Garrett MD, Yeo M, et al. Rho kinase inhibitors block melanoma cell migration and inhibit metastasis. Cancer Res. 2015; 75:2272–84. [PubMed: 25840982]

29. Strozyk EA, Desch A, Poeppelmann B, Magnolo N, Wegener J, Huck V, et al. Melanoma-derived IL-1 converts vascular endothelium to a proinflammatory and procoagulatory phenotype via NFkappaB activation. Exp Dermatol. 2014; 23:670–6. [PubMed: 25041487]

30. Reichel CA, Khandoga A, Anders HJ, Schlondorff D, Luckow B, Krombach F. Chemokine receptors Ccr1, Ccr2, and Ccr5 mediate neutrophil migration to postischemic tissue. J Leukoc Biol. 2006; 79:114–22. [PubMed: 16275892]

31. Schrage A, Loddenkemper C, Erben U, Lauer U, Hausdorf G, Jungblut PR, et al. Murine CD146 is widely expressed on endothelial cells and is recognized by the monoclonal antibody ME-9F1. Histochem Cell Biol. 2008; 129:441–51. [PubMed: 18214516]

32. Roblek M, Strutzmann E, Zankl C, Adage T, Heikenwalder M, Atlic A, et al. Targeting of CCL2-CCR2-Glycosaminoglycan Axis Using a CCL2 Decoy Protein Attenuates Metastasis through Inhibition of Tumor Cell Seeding. Neoplasia. 2016; 18:49–59. [PubMed: 26806351]

33. Abraham S, Yeo M, Montero-Balaguer M, Paterson H, Dejana E, Marshall CJ, et al. VE-Cadherin-mediated cell-cell interaction suppresses sprouting via signaling to MLC2 phosphorylation. Curr Biol. 2009; 19:668–74. [PubMed: 19345098]

34. Karassek S, Starost L, Solbach J, Greune L, Sano Y, Kanda T, et al. Pertussis Toxin Exploits Specific Host Cell Signaling Pathways for Promoting Invasion and Translocation of Escherichia coli K1 RS218 in Human Brain-derived Microvascular Endothelial Cells. J Biol Chem. 2015; 290:24835–43. [PubMed: 26324705]

35. Zhao L, Lim SY, Gordon-Weeks AN, Tapmeier TT, Im JH, Cao Y, et al. Recruitment of a myeloid cell subset (CD11b/Gr1(mid))via CCL2/CCR2 promotes thedevelopment of colorectal cancer liver metastasis. Hepatology. 2013; 57:829–39. [PubMed: 23081697]

36. Nywening TM, Wang-Gillam A, Sanford DE, Belt BA, Panni RZ, Cusworth BM, et al. Targeting tumour-associated macrophages with CCR2 inhibition in combination with FOLFIRINOX in patients with borderline resectable and locally advanced pancreatic cancer: a single-centre, open-label, dose-finding, non-randomised, phase 1b trial. Lancet Oncol. 2016; 17:651–62. [PubMed: 27055731]

37. Roberts TK, Eugenin EA, Lopez L, Romero IA, Weksler BB, Couraud PO, et al. CCL2 disrupts the adherens junction: implications for neuroinflammation. Lab Invest. 2012; 92:1213–33. [PubMed: 22641100]

38. Stamatovic SM, Keep RF, Mostarica-Stojkovic M, Andjelkovic AV. CCL2 regulates angiogenesis via activation of Ets-1 transcription factor. J Immunol. 2006; 177:2651–61. [PubMed: 16888027]

39. Roodhart JM, He H, Daenen LG, Monvoisin A, Barber CL, van Amersfoort M, et al. Notch1 regulates angio-supportive bone marrow-derived cells in mice: relevance to chemoresistance. Blood. 2013; 122:143–53. [PubMed: 23690447]

40. Vestweber D. How leukocytes cross the vascular endothelium. Nat Rev Immunol. 2015; 15:692–704. [PubMed: 26471775]

41. Garcia-Roman J, Zentella-Dehesa A. Vascular permeability changes involved in tumor metastasis. Cancer Lett. 2013; 335:259–69. [PubMed: 23499893]

42. Vandenbroucke E, Mehta D, Minshall R, Malik AB. Regulation of endothelial junctional permeability. Ann N Y Acad Sci. 2008; 1123:134–45. [PubMed: 18375586]

43. Reymond N, d'Agua BB, Ridley AJ. Crossing the endothelial barrier during metastasis. Nat Rev Cancer. 2013; 13:858–70. [PubMed: 24263189]

44. Vicente-Manzanares M, Ma X, Adelstein RS, Horwitz AR. Non-muscle myosin II takes centre stage in cell adhesion and migration. Nat Rev Mol Cell Biol. 2009; 10:778–90. [PubMed: 19851336]

45. Roblek M, Calin M, Schlesinger M, Stan D, Zeisig R, Simionescu M, et al. Targeted delivery of CCR2 antagonist to activated pulmonary endothelium prevents metastasis. J Control Release. 2015; 220:341–7. [PubMed: 26522070]
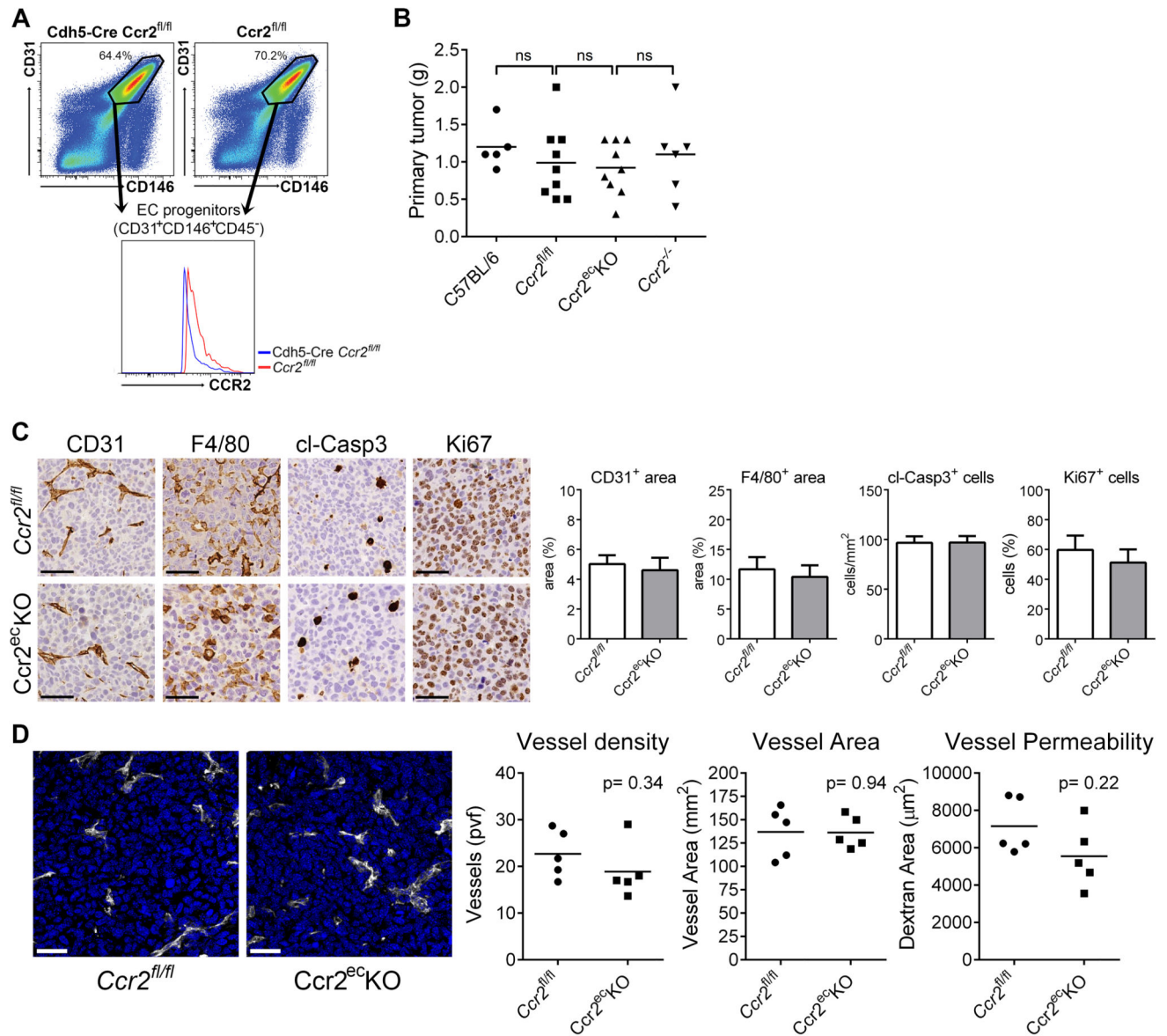
Figure 1. Primary tumor growth was not effected by endothelial deficiency of CCR2.
A) Analysis of endothelial progenitor cells (CD31+CD146+CD45-) in the lungs of naïve Ccr2ecKO mice and *Ccr2fl/fl* mice. **B)** Weight of primary subcutaneous LLC1.1 tumors at time of resection (14 days after implantation); ns = not significant. **C)** Representative images of primary tumors stained with CD31, F4/80, cl-Casp3 and Ki67 Abs together with histological analysis, respectively. Bar = 50 μm. **D)** Representative images of primary tumors from Ccr2ecKO and *Ccr2fl/fl* mice, respectively, stained with anti-CD31 (white) to analyze vascular density (nuclear staining with DAPI = blue). The analysis of vessel density and the vessel area revealed no difference between mice of both genotypes. Vessel permeability in tumors was determined using intravenous injection of dextran-FITC 1 h prior to termination. Cryosections of the tumors were analyzed for the dextran-FITC. Bar = 30 μm.
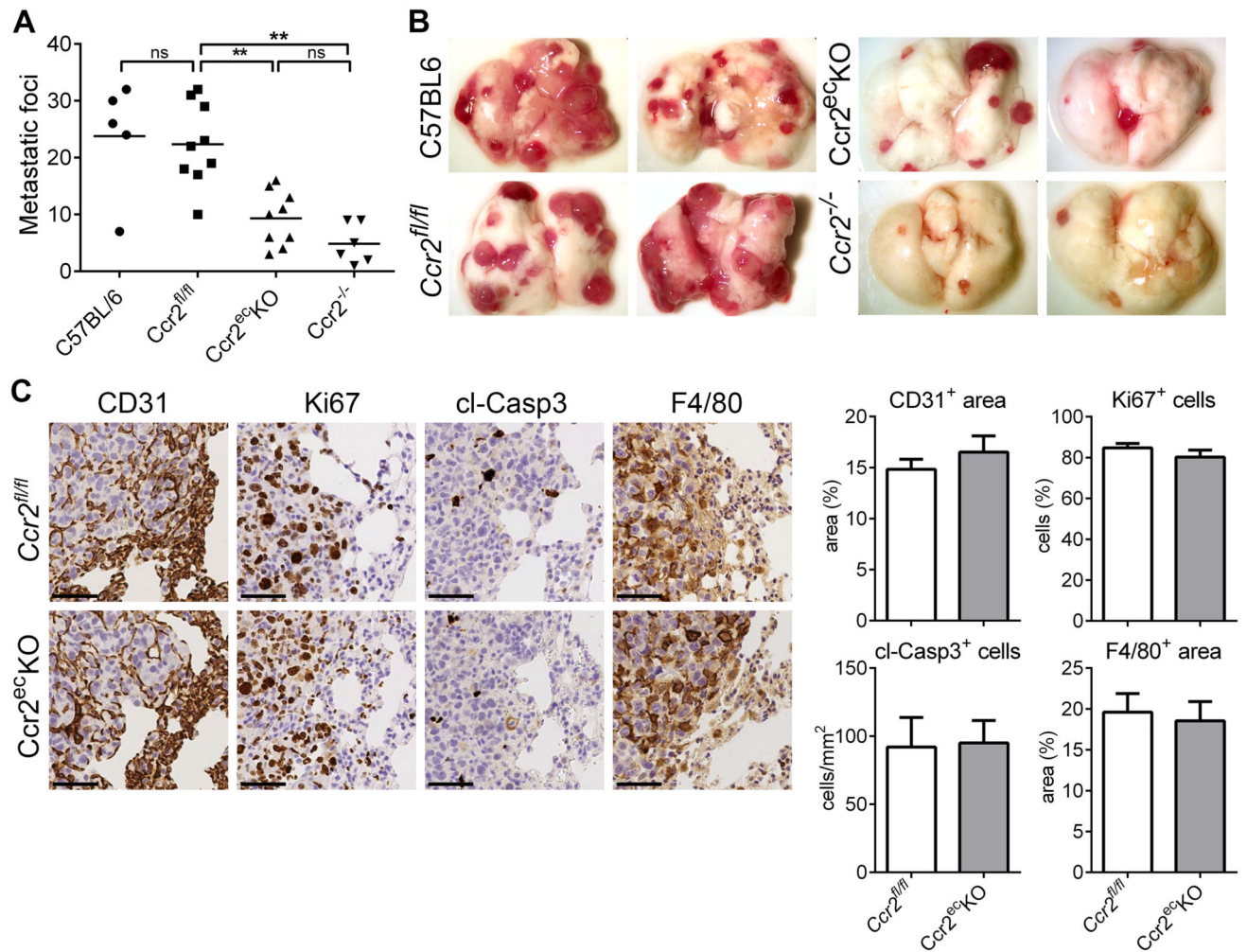
Figure 2. Endothelial Ccr2 is required for lung metastasis.
A) Spontaneous lung metastasis in C57BL/6, *Ccr2*$^{fl/fl}$, Ccr2^{ec}KO, and *Ccr2*$^{-/-}$ mice 28 days after subcutaneous injection of LLC1.1 cells. **; p<0.01; ns = not significant. **B)** Representative images of lungs from mice analyzed in panel A**. C)** Representative images of pulmonary metastasis stained with anti-CD31 (vasculature) and anti-F4/80 (macrophages) antibodies. Proliferating cells (Ki67 staining) and apoptotic cells (cleaved Caspase 3 staining; cl-Casp3) were evaluated. The edge of a metastatic lesion is presented. The histological analysis of metastatic foci only was performed. Bar = 50 μm.
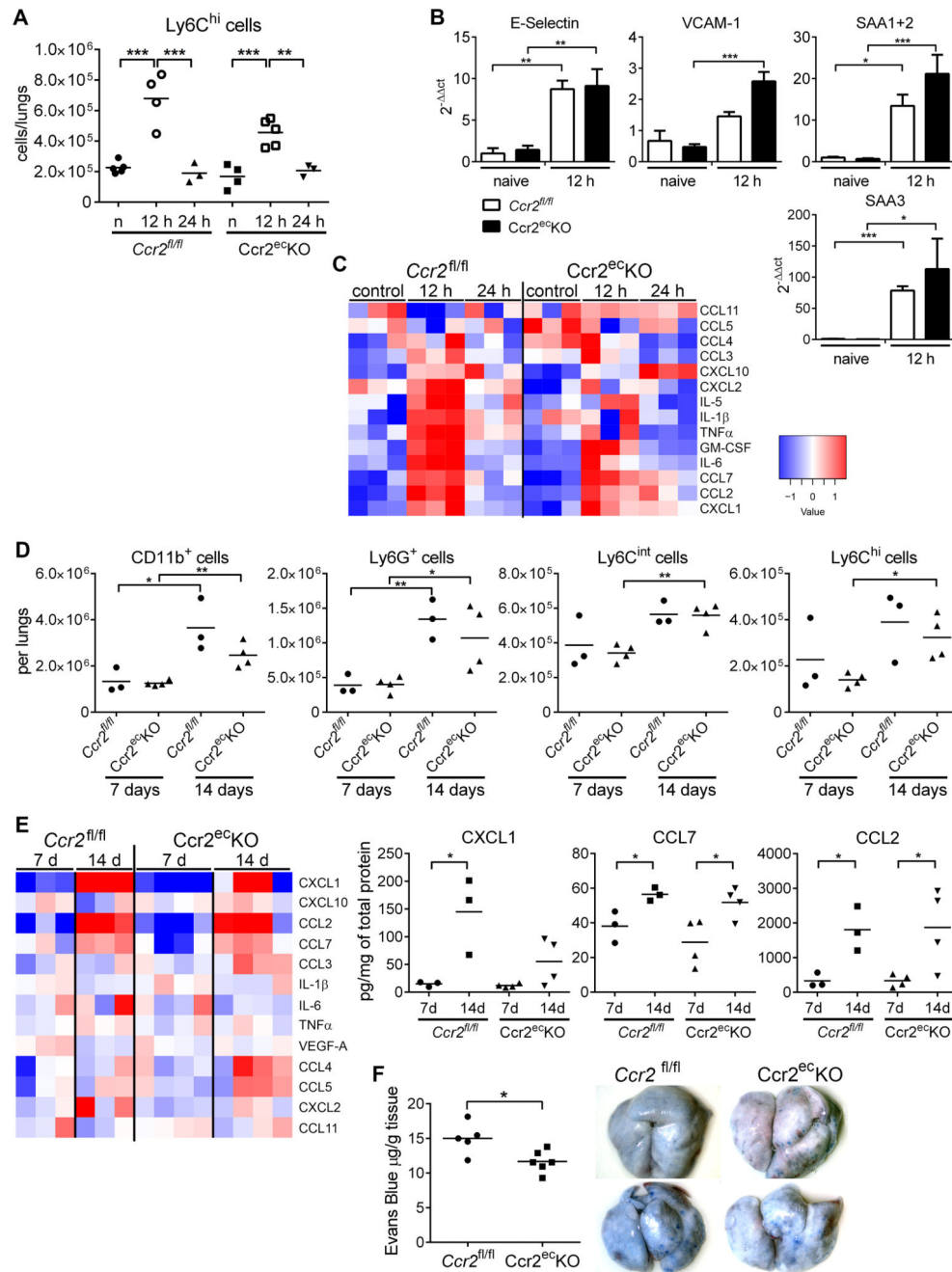
Figure 3. Initiation of the pre-metastatic niche is not impaired in Ccr2ecKO mice.
A) Flow cytometry analysis of inflammatory monocytes (CD45+CD11b+Ly6G-Ly6Chi) recruited to the lungs at 12 and 24 h after i.v. MC-38GFP injection of *Ccr2fl/fl* and Ccr2ecKO mice. Untreated naïve mice (n) were used as controls. **B)** Endothelial cells (CD45-CD11b-CD31+) sorted from lungs of *Ccr2fl/fl* and Ccr2ecKO mice 12 h after i.v. MC-38GFP injection or untreated (naive) mice were analyzed for the expression levels of E-selectin, VCAM-1, SAA1+2 and SAA3 (n = 3-6) **C)** Amounts of cytokines in perfused lung homogenates of *Ccr2fl/fl* and Ccr2ecKO mice at 12 and 24 h after i.v. MC-38GFP injection.

Untreated mice (control) were used as controls. **D)** Flow cytometry analysis of myeloid cells (CD45$^+$CD11b$^+$), granulocytes (CD45$^+$CD11b$^+$Ly6G$^+$), Ly6C^{int} monocytes (CD45$^+$CD11b$^+$LyG$^-$Ly6C^{int}), and inflammatory monocytes (CD45$^+$CD11b$^+$Ly6G$^-$Ly6C^{hi}) recruited to lungs of mice s.c.-injected with LLC1.1 cells after 7 and 14 days. **E)** Amounts of cytokines detected in lung homogenates of mice s.c.-injected with LLC1.1 cells after 7 and 14 days. **F)** Lung vascular permeability assay of *Ccr2$^{fl/fl}$* and Ccr2^{ec}KO mice 14 days after s.c. injection of LLC cells, including representative macroscopic images. Statistical significance in panels B, D, E and F was assessed using unpaired t-test; *; p<0.05; **; p<0.01; ***; p<0.001.
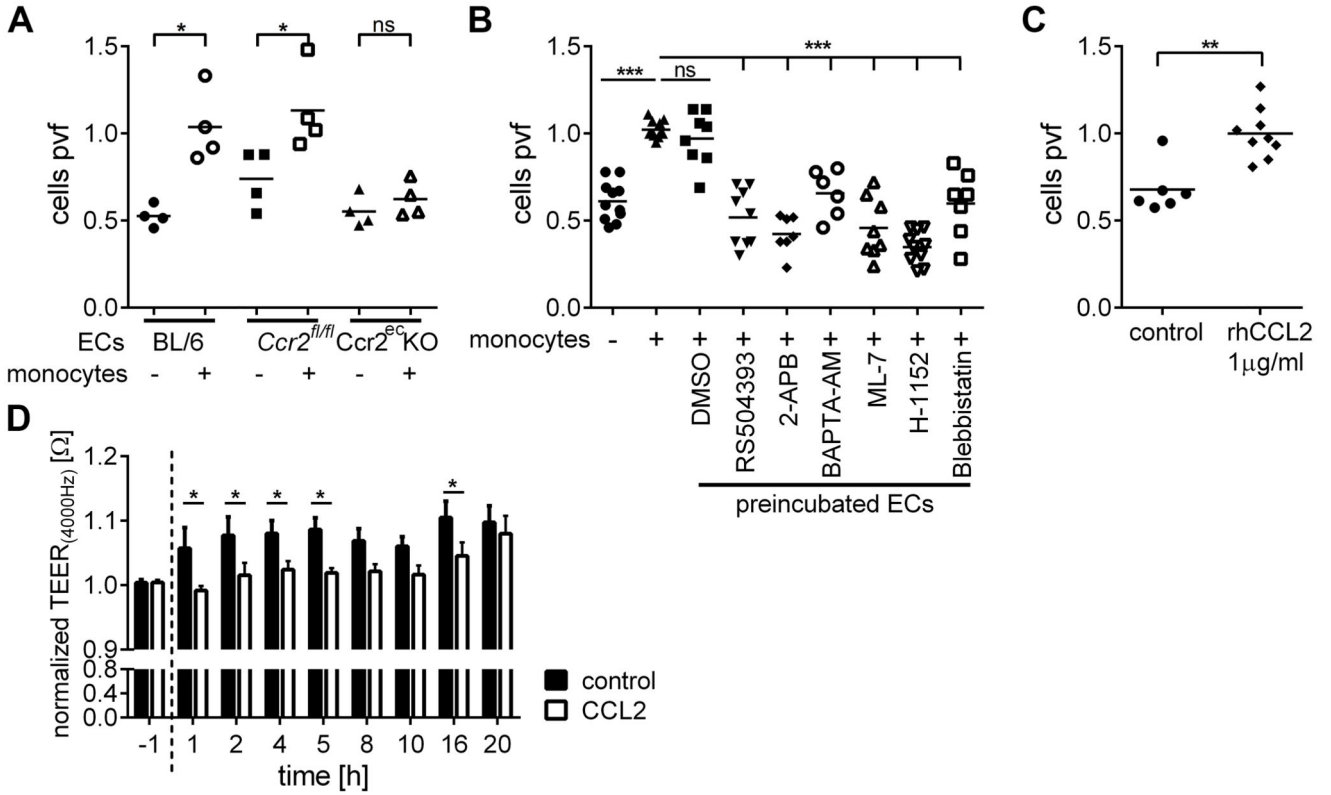
Figure 4. CCL2 stimulation induces endothelial retraction and transendothelial migration of tumor cells.

A) Transendothelial migration of MC-38GFP cells through lung endothelial cells isolated from C57BL/6 wild-type (BL6), *Ccr2*^{fl/fl} and Ccr2[ec]KO mice, either in the absence (-) or in the presence of CD115^{+} monocytes (+).The number of migrated tumor cells was counted per view field (pvf) and is normalized to the control (+ monocytes); ns; not significant; *; p<0.05. **B)** Transendothelial migration of MC-38GFP cells in the absence (-) or in the presence of CD115^{+} monocytes (+). Endothelial cells from C57BL/6 mice (ECs) were pre-treated with RS-504393 (50 μM), 2-APB (50 μM), BAPTA-AM (10 μM), ML-7 (1 μM), H-1152 (5 μM), and Blebbistatin (2.5 μM) for two hours and washed out of the inhibitor prior to addition of tumor cells +/- monocytes. DMSO as a diluent of inhibitors was used as a control. Tumor cell migration was analyzed as described in panel A. ***; p<0.001. **C)** Transendothelial migration of MC-38GFP cells (without monocytes) only in presence of rhCCL2 (1 μg/ml) compared to a control. **; p<0.01. **D)** TEER measurement of primary lung endothelial cells upon stimulation with rhCCL2 (10 μg/ml). TEER values for rhCCL2-treated and control samples were normalized to 1 at the start of stimulation (0 h). Black bars = control; open bars = CCL2-treated; n = 4; *; p<0.05; other time points showed no significant differences.
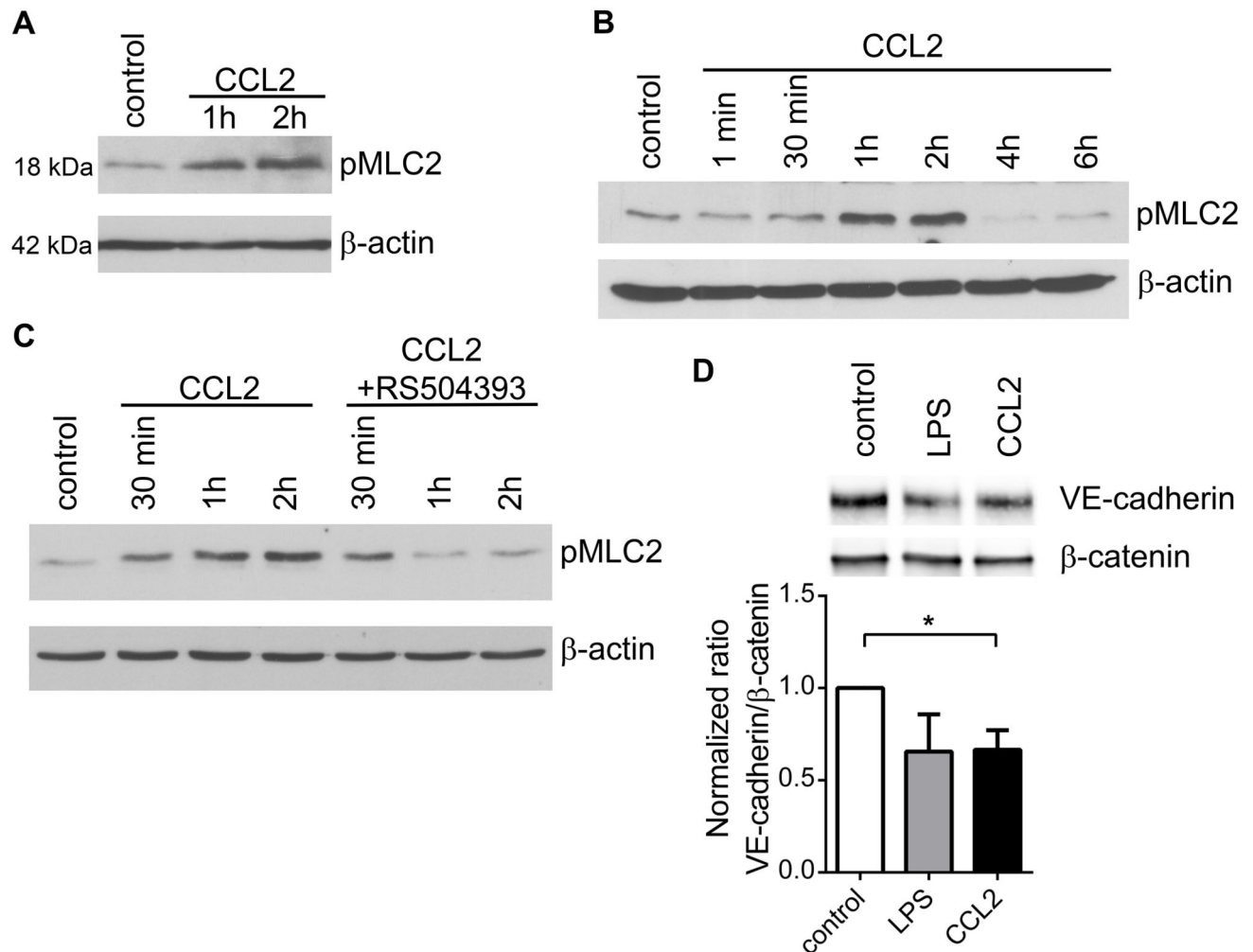
Figure 5. CCL2 stimulation of endothelial cells induces phosphorylation of myosin-light chain 2 and loosening of endothelial barrier.
A) Immune-detection of phosphorylated MLC2 (pMLC2) in the lysates of primary pulmonary endothelial cells after stimulation with CCL2 (100 ng/ml) for one and two hours. Per lane 20 μg of protein lysate were loaded; β-actin served as a loading control. **B)** Detection of pMLC2 in bEnd.3 endothelial cells after stimulation with CCL2 (100 ng/ml). β-actin serves as a loading control. **C)** Immune-detection of pMLC2 in lysates of bEnd.3 endothelial cells stimulated with CCL2 (100 ng/ml) for 30 min, 1 h, and 2 h, in the absence or presence of the CCR2 inhibitor RS504393 (50 μM). Per lane 20 μg of protein lysate were loaded; β-actin served as a loading control. **D)** Immunoprecipitation of β-catenin and detection of co-immune-precipitated VE-cadherin in bEnd.3 cell lysates stimulated with rhCCL2 (1 μg/ml) for 1 h. Quantification of immune-precipitated VE-cadherin in ratio to β-catenin (lower panel) n=4, *; p<0.05.